Study on energy absorption capacity of carbon fiber tube

Liu Yuhao, Gu Haiming, Ren Jiwei, Wang Xu

(China Automotive Technology and Research Center Co.,Ltd, Tianjin, China)

*Corresponding author's e-mail: 1370786276@qq.com

Abstract. In order to study the energy absorbing capacity of carbon fiber pipe in collision, a material test bench was designed with the help of collision sled. The influence of induced holes on the mechanical properties of carbon fiber sample was studied. Through two different ways of collision, the torn and bending energy absorbing capacity of the carbon fiber square tube was obtained, and the way to increase the energy absorption capacity of the carbon fiber square tube was discussed.

1. Introduction

With the development trend of automotive lightweight, how to improve automobile performance and reduce the weight of automobiles has become the greatest concern of major automobile manufacturers [1-2]. Carbon fiber materials have the characteristics of high strength, light weight and corrosion resistance. Carbon fiber and its fabric are light and bendable, able to fit different component shapes, and considerably convenient to form [3-4]. In the automotive industry, it is often used to make car body panels, replacing traditional sheet metal parts; or used to manufacture complex aerodynamic components to improve car performances of dynamic and maneuverability [5-6]. Due to its excellent physical and chemical properties, the application prospect is very broad.

In practical applications, the mechanical properties and energy absorption capacity of carbon fiber materials under high-speed impact are difficult to obtain directly, which brings about great difficulties for the design of vehicles energy adsorption structures. Aiming at this situation, in this paper a material test bench was designed and utilized to relevant test. The influence of induced pores was explored, and the calculation method of carbon fiber square tube energy absorption capacity was provided, making a reference for the design of carbon fiber structure.

2. Material test beach

In order to obtain the response of carbon fiber materials under the impact, a test bench for carbon fiber material was designed by means of an accelerated collision vehicle, the schematic diagram of which is shown in Figure 1. Thereinto, 1 is the test bench body; 2 is a rubber block to protect the rear; 3 is the sliding table, 3.1 is the protective surface, 3.2 is the end face of the sliding table rear, 3.3 is the threaded hole for counterweight mounting, 3.4 is the material impacting surface; 4 is the linear guide rail; 5 is the test material; 6 is a rubber block to protect the front end; 7 is the four-jaw chuck. An acceleration sensor is attached to the rear-end surface of the sliding table to collect the acceleration of the sliding table 3 in the test. The real test beach is shown in Figure 2.

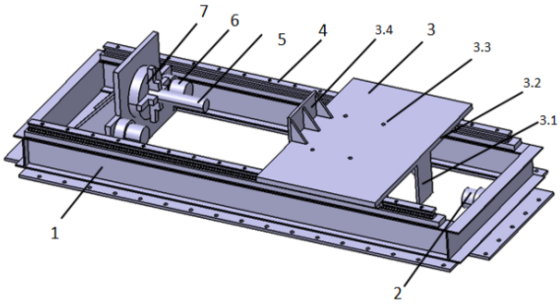

Figure 1. schematic diagram of test beach

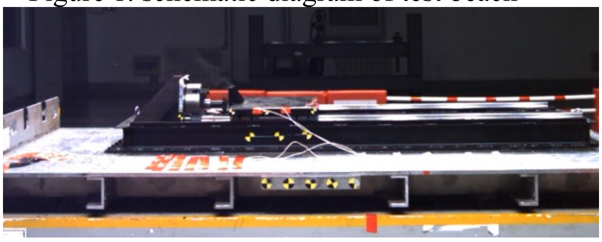

Figure 2. Practical image of material test beach

During the test, the material sample hit the impact surface at a uniform speed, resulting in the vehicle (sample) accelerating first and then moving at a constant speed. The acceleration is displayed in Figure 3. The acceleration distance of the vehicle could be obtained by integral, which was also the reserved distance between the end plane of the test material and the material impacting surface, calculated by the Equation (Eq.) 1.

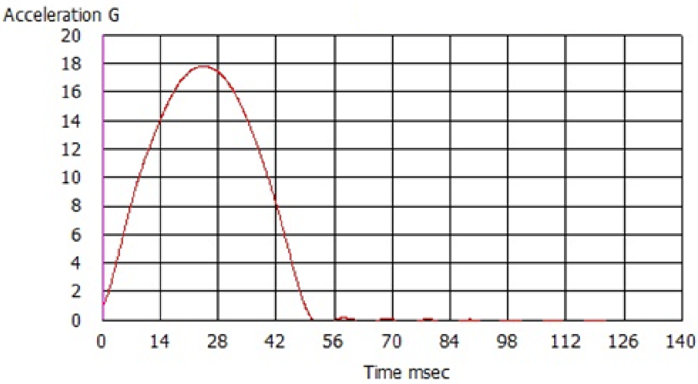

Figure 3. Acceleration curve of the vehicle

$$S = \iint_0^t a dt \qquad \text{(Eq. 1)}$$

where a is the acceleration of the vehicle, S is the displacement of the vehicle, and t is the end time of the vehicle acceleration.

3. Study on influence of induced holes on the mechanical properties of carbon fiber material

The process parameters of the carbon fiber material used in this paper were: square cross section, outside length of 40mm, tube wall thickness of 1.5m, 7-layers plain cloth layer, carbon fiber direction of 0° and 90°, epoxy resin in prepreg, and autoclave molding. In order to facilitate the study of the effect of induced pores on the mechanical properties of carbon fibers, a round tube sample was used for the test.

Three different types of slotted carbon fiber tubes were selected, respectively named A (the number of axial induction slots was 3, the number of radial induction slots was 4), B (the number of axial induction slots was 3, and the number of radial induction slots was 2), and C (no induction slot). The specific dimensions are shown in Figure 4. In the test, the mass of the counterweight block was 78kg, the impact speed was 20km/h, and the maximum acceleration of the vehicle was18g. The vehicle curve is shown in Figure 3.

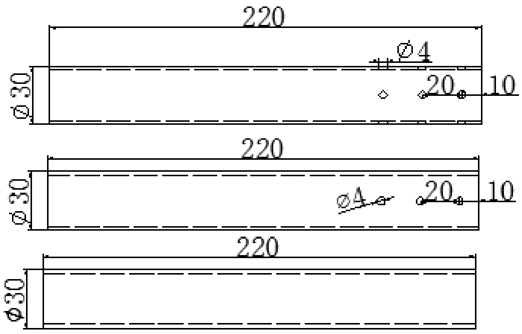

Figure 4. Dimensions of carbon fiber tubes

Through the test, the acceleration-time curves of the vehicle and the impact surface could be directly acquired, and the displacements of the vehicle and the impact surface could be respectively obtained by Eq. 2, followed by an acquisition of the relative displacement, namely crumple length of the sample. Eq. 3 was utilized to draw the force-time curve of the material, thereby obtaining the force-displacement curve of the material, shown as Figure 5. The status of the sample is presented in Figure 6. As can be seen in the figure, the tearing of the three carbon fiber samples is basically the same and their coincidence of the acceleration-displacement curves are comparatively high, without big fluctuations. Therefore, it is considered that the opening of the induced pores has less effect on the tearing and mechanical properties of the carbon fibers.

$$S(t) = \iint_0^t a(t)dt \quad \text{(Eq. 2)}$$

$$F(t)=M*a(t) \quad \text{(Eq. 3)}$$

where S(t) is the displacement of the vehicle (impact surface), a(t) is the acceleration of the vehicle (impact surface), F(t) is the force on the impact surface (sample), M is the counterweight of the impact surface

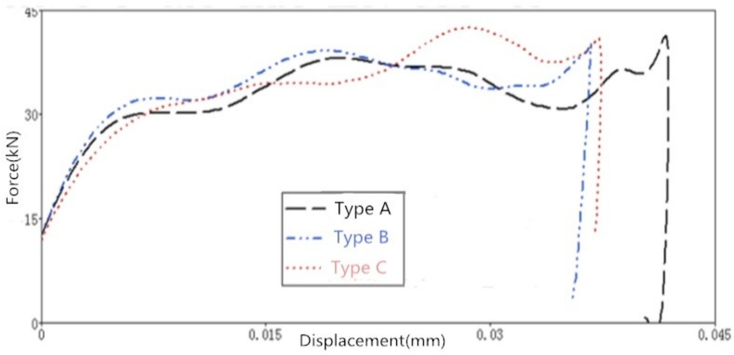

Figure 5. Mechanical properties of different carbon fiber tubes

(a) Tearing of type A carbon fiber

(b) Tearing of type B carbon fiber

(c) Tearing of type C carbon fiber

Figure 6. Tearing of different carbon fiber tube

4 Study on energy absorption capacity of carbon fiber tubes

4.1 Determination of test scheme

Carbon fiber crumple adsorbed energy mainly through two ways, torn energy absorption and plane bending energy absorption. For the convenience of research, the square tube was selected for experiment. Two test approaches were designed as below. Scheme 1: The material sample was cut with the horizontal plane of the four-jaw chuck jaw as the fixed surface and the vertical surface as the cutting surface. Under the circumstances, 8 torn edges appeared, and the bending side length was 100mm (the sum of the chuck jaw cutting surfaces); Scheme 2: the chuck was replaced by a fixed block, with 4 torn edges of the material sample impacted by a plane and the bending side length of 240mm (the collision plane is the collision surface). The two experimental schemes are shown in Figure 7. The test sliding beach had a counterweight of 78kg, at a speed of 20km/h, and its acceleration curve is illustrated by Figure 3. The status of the material sample after the test is presented in Figure. 8.

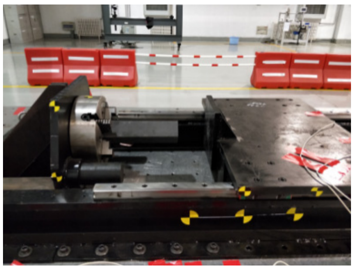

(a) Test scheme 1

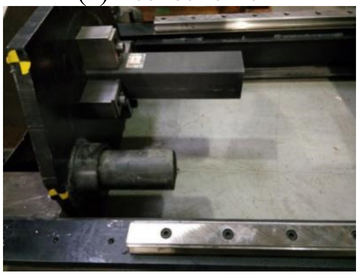

(b) Experiment scheme 2

Figure 7. Test schemes

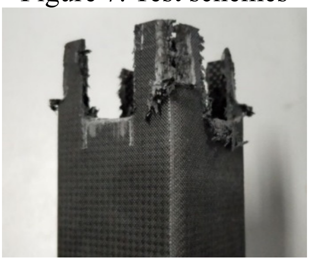

(a) The sample after test by scheme 1

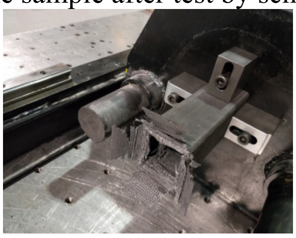

(b) The sample after test by scheme 2

Figure 8. Samples after test

4.2 Test data verification

For the purpose to verify the reliability of the beach acceleration curve, the vehicle and the sliding beach were verified by the test data, to determine the reliability of the test results. The verification way is as shown in Eq. 4:

$$D_{crumple}=D_{vehicle}-D_{sliding\ beach} \quad \text{(Eq. 4)}$$

where $D_{crumple}$ is the crumple distance of the carbon fiber sample, $D_{vehicle}$ is the vehicle displacement during the crumple process of the carbon fiber material. $D_{sliding}$ beach is the displacement of the carbon fiber material.

The displacement of the test vehicle was calculated by Eq.5.

$$D_{vehicle}=D_{vehicle\ total}-D_{vehicle\ acceleration} \quad \text{(Eq. 5)}$$

where $D_{vehicle}$ total is the total displacement of the vehicle in the test (obtained by twice integral of the vehicle acceleration); $D_{vehicle}$ acceleration is the displacement of the vehicle before collusion with the sliding beach (obtained by twice integral of the vehicle acceleration).

The displacement of the sliding beach is obtained by twice integrations of its acceleration. The crumple distance of the carbon fiber sample was calculated and displayed in Figure 9, and the maximum compression of the carbon fiber is 36.05 mm. The actual amount of compression (measured value) was 35.90 mm, as shown in Figure 10. Owing to high goodness of fit of the calculated value and the practically measured value, the calculated values were adopted to calculate the material parameters in the subsequent calculations. The verification process of scheme 2 was the same as that of scheme 1, with the calculated value of 36.01 mm and the actual measured value of 35.80 mm.

The force-displacement curve of the materials in the two schemes was determined by utilization the crumple curve of the carbon fiber samples and the acceleration curve of the sliding beach, exhibited in Figure 11. As seen in the figure, in the two schemes, the carbon fibers are stable at the crumple stage (after the second peak), and the force-displacement curves are basically consistent.

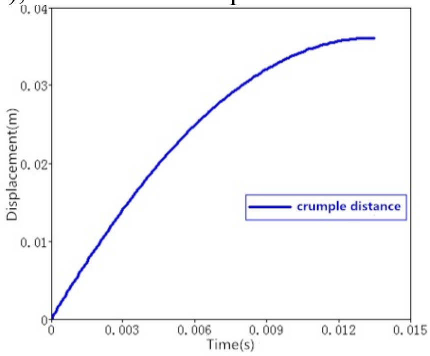

Figure 9. Compression of carbon fiber

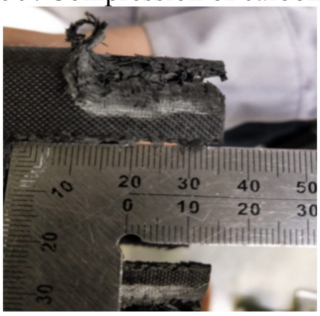

Figure 10. Actual compression distance

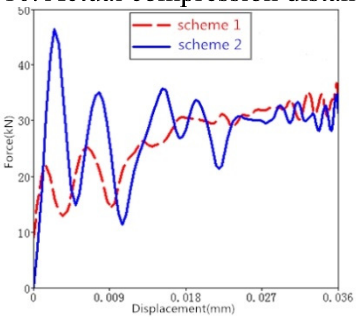

Figure 11. Force-displacement curves of the two schemes

4.3 Reverse calculation of energy absorption capacity of carbon fiber

The main energy absorption ways of carbon fiber are torn and plane bending adsorption. Therefore, we hoped to obtain the torn and bending energy absorption capacity of the test sample through experiments. Relying on the test curve, Eq. 6 was obtained.

$$D_1 * \int_0^{S_1} f(s)_{tear\ force}\, ds + \int_0^{S_1} H_1 f(s)_{bend\ force}\, ds = \frac{1}{2} m v_1^2$$

$$D_2 * \int_0^{S_2} f(s)_{tear\ force}\, ds + \int_0^{S_2} H_2\, f(s)_{bend\ force} ds = \frac{1}{2} m v_2^2 \qquad \text{(Eq. 6)}$$

$f(s)_{tear\ force}ds = Q_{tear}$
$f(s)_{bend\ force}ds = Q_{bend}$

where D_1 is the number of sample torn edges of the in scheme 1, D_1=8; S_1 is the sample crumple distance in scheme 1, S_1=0.03605m; H_1 is the total width of the sample plane bending in scheme 1, H_1=0.1m; D_2 is the number of sample torn edges of the in scheme 2, D_2=4; S_2 is the sample crumple distance in scheme 2, S_2=0.03601m; H_2 is the total width of the sample plane bending in scheme 2, H_1=0.24m; f(x)tear force is the tearing force function of the sample displacement; f(x)bend force is the bending force function of the sample displacement in a unit plane width; m is the total weight of the sliding beach, m = 78kg; Q_{tear} is the energy required to tear the sample of unit distance, namely torn energy absorption capacity; Q_{bend} is the energy required to bend the sample of unit distance at the unit width, namely the bending energy absorption capacity; V_1 is the maximum speed of the sliding beach in Scheme 1 (obtained by intergral of the acceleration of the sliding beach);V_2 is the maximum speed of the sliding beach in Scheme 2 (obtained by intergral of the acceleration of the sliding beach).

Solution of Eq.6 could access to the torn energy absorption capacity Q_{tear} of 974.36J, when the material underwent a unit length tearing; the bending energy absorption capacity Q_{bend} was 25.64J.

On account of Q_{tear} /Q_{bend}=38, when the side length of the carbon fiber square tube was 38 mm and the carbon fiber tube underwent a unit distance tearing, the torn energy adsorption and the bending energy absorption were equal, that was Q_{tear}=38Q_{bend}. When the side length of the carbon fiber tube was longer than 38mm, the torn energy adsorption was greater than the bending energy absorption. When the side length of the carbon fiber tube was shorter than 38mm, the torn energy adsorption was smaller than the bending energy absorption.

Meanwhile, Q_{tear} and Q_{bend} are constant for a specific carbon fiber material, so the energy absorption equation of the carbon fiber tube material can be described as Eq. 7.

$$(DQ_{tear}+HQ_{bend})\ S=Q \qquad \text{(Eq. 7)}$$

where D is the sides number of the carbon fiber tube, H is the bending side length of the carbon fiber tube, S is the torn distance of the carbon fiber tube, and Q is the total energy absorbed.

It can be seen from Eq. 7 that, with the increase of the bending side length of the carbon fiber tube, H(D)enlarges, while the total energy has no change, which results in the decrease of the crumple distance. Here ($DQ_{tear}+HQ_{bend}$) is considered as the whole energy absorption capacity of the carbon fiber tube.

4.4 Design for increasing the energy absorption capacity of materials

Through the foregoing analysis, the bending and torn energy adsorption capacities of the materials during the crumple process were obtained, and the whole energy absorption capacity of the carbon fiber tube were defined. In order to increase the whole energy absorption capacity of the material during the crumple process, a polygonal carbon fiber square tube (simultaneously increasing the circumference and the sides number of the carbon fiber tube) was designed. The cross section is shown in Figure 12. This polygonal square tube has 12 sides, with a total circumference of 284 mm. Under the test conditions same as those set in the above description, the counterweight of the test sliding beach was 78kg, at a target speed of 20km/h, and the test results are exhibited in Figure 13.

Figure 12. Sectional view of the polygonal square tube

(a) Sample test result

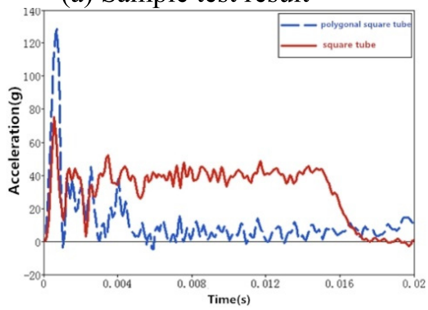

(b) Test acceleration curve

Figure 13. Test results of polygonal carbon fiber tube

Through the experiments it was found that, when the circumference and the sides number of the carbon fiber tube were increased, the polygonal carbon fiber square tube did not suffer axial crumple in the tests, but undergo radial tearing, and nested together. As can be seen from the acceleration curve of Figure 13, when the circumference and the sides number increase, the first peak of the acceleration curve enlarges significantly, indicating that the axial stiffness of the polygonal square tube is also improved significantly. When the axial stiffness of the square tube exceeds the radial stiffness, the carbon fiber tube will be radially torn, and when the carbon fiber is radially torn and broken, the sliding beach acceleration curve will sharply decline, with a great reduction of energy absorption property. Therefore, for the purpose to ensure the good energy absorption property of the carbon fiber tube, its circumference and sides number are required to be rationally designed.

5. Conclusions

In order to explore the mechanical properties of carbon fiber materials, in this paper a material test bench was designed to test carbon fiber samples, and relevant conclusions were acquired.

(1) The induced holes had less effect on the mechanical properties of carbon fiber materials.

(2) Both tear and bend of carbon fiber material can absorb the collision energy. The energy absorption capacity of carbon fiber structures can be obtained by test data.

(3) For the purpose to ensure the good energy absorption property of the carbon fiber tube, its circumference and sides number are required to be rationally designed.

References

[1] Zhao Yanrong, Hu Ping, Liang Jicai. Application of Carbon Fiber Composites in the Automotive industry[J]. China Synthetic Resin and Plastics, 2015, 32(5):95-98.

[2] Chen Linshan, Chen Xiang. Application of Plastics and Composite Materials in Lightweight Design of Automobile[J]. China Plastics Industry, 2017, 45(7):103-106.

[3] Zhang Xinyuan, He Bixia, Li Jianli. Property and Application of High-performance Carbon Fiber[J]. Cotton Textile Technology, 2011, 39(4):65-68.

[4] Han Keqing, Yan Bin, Tian Yincai. Low Cost Preparation Technology of Carbon Fiber and Composite Materials[J]. Materials China, 2012, 31(10):30-36.

[5] Li Jianfeng. Application Prospects Carbon Fiber Materials in Auto-motive Parts[J]. Chin Sci Tech Panoram Maga, 2015(21):76.

[6] Wang Dongchuan, Niu Qizhi, KeFeng, Application of Carbon Fiber Reinforced Composites in Automobiles[J]. Auto Tech Mater, 2005(4):33-36.